View metadata, citation and similar papers at core.ac.uk
brought to you by CORE
provided by NASA Technical Reports Server

A PROCEDURE FOR ESTIMATION OF SEA-SURFACE TEMPERATURE FROM REMOTE MEASUREMENTS IN THE 10 - 13 μm SPECTRAL REGION

M-4

By David C. Anding, Science Applications, Inc., La Jolla, California

ABSTRACT

This paper demonstrates the feasibility of a procedure for the remote measurement of sea-surface temperature which inherently corrects for the effect of the intervening atmosphere without recourse to climatological data. The procedure relies upon the near-linear differential absorption properties of the infrared window region between 10 and 13 μm and requires radiometric measurements in a minimum of two spectral intervals within the infrared window which have a significant difference in absorption coefficient. The procedure has been applied to Nimbus 4 infrared interferometer spectrometer (IRIS) data and to Skylab EREP S191 spectrometer data, and it is demonstrated that atmospheric effects on the observed brightness temperature can be reduced to less than 1.0 Kelvin.

INTRODUCTION

Global measurement of sea-surface temperature (hereafter referred to as SST) on a daily basis is currently operational at NOAA's National Environmental Satellite Service (NESS) Center. SST data are archived after a rather complex analysis of data from the scanning radiometer (SR) aboard the NOAA-4 satellite. The procedure for extracting SST information from SR data is an extension of that of Smith and Rao [1]. Basically, infrared window measurements (10.5 - 12.5 μm) are converted to SST values, at degraded spatial resolution, with proper consideration of SR instrument noise, noise related to signal transmission, receiving, and processing, and after accounting for the effects of the intervening atmosphere based upon climatological data.

Because of inherent limitations in the single-channel scanning radiometer method of producing SST's, archived temperatures have limited accuracy and spatial resolution. The next generation of TIROS satellites, denoted TIROS-N series, will contain a five-channel advanced very high resolution radiometer (AVHRR), which will provide for improved SST retrieval. The first instrument to be flown, planned for FY 78, will contain four channels, with a fifth channel to be added on the fourth or fifth satellite in the TIROS-N series. The nominal spectral regions for each of the five channels are 0.55 to 0.9 μm, 0.72 μm to detector cutoff (approximately 1.0 μm), 3.55 to 3.93 μm, 10.5 to 11.5 μm, and 11.5 to 12.5 μm, which will be the fifth channel to be added. The spectral response of the first four channels has been finalized, however, the spectral response of the fifth channel is still open. Of major impact to SST measurement is the addition of the infrared channel from 3.55 - 3.93 μm and the division of the present infrared window channel, i. e., 10.5 - 12.5 μm, into two channels. The reason for the addition of the two infrared channels is to provide additional information to correct for the effects of atmospheric moisture on the observed radiance (which can be significant, particularly for warm and moist conditions) without recourse to climatological data.

Previous studies [2, 3, 4, 5] have indicated that the addition of a second channel in the infrared window, one somewhat less transparent than the other, would allow for compensation of the effects of absorption and emission by atmospheric water vapor without recourse to climatological or other supportive data. The investigations involved the use of radiative transfer models, and large field-of-view space acquired data, i. e., the

infrared interferometer spectrometer (IRIS) aboard Nimbus 4. Although the results were encouraging, they remain tentative until they can be verified by an experiment for which the sensor field-of-view is comparable to that which will be used on future TIROS satellites. The Skylab mission provided the first opportunity for such a verification experiment.

This paper describes the results of an investigation which utilized IRIS and S191 spectrometer data acquired during two of the three Skylab missions to validate the radiative transfer models used in the initial investigations, and test the validity and correctness of two-channel temperature estimating algorithms developed from the radiative transfer models. The results of the investigation indicated that a significant benefit will be derived by the addition of a second channel in the infrared window region. Specifically, without recourse to climatological data, the investigation indicated SST's could be estimated to within $1^{\circ}K$.[1] Although the spectral bands selected for the analysis yielded a satisfactory result, the investigation also indicated that the infrared window transmission function contains nonlinearities and uncertain aerosol effects which could have a significant impact upon the optimum choice of the two spectral channels. Since the present analysis was limited in scope it is recommended that a further analysis be performed before a final choice of spectral channels is made.

THEORETICAL BASIS OF REMOTE SST MEASUREMENT AT THERMAL INFRARED WAVELENGTHS

The spectral radiance emitted by an opaque body at wavelength λ is given by

$$L(\lambda, T) = \epsilon(\lambda) L^{bb}(\lambda, T) \tag{1}$$

where $\epsilon(\lambda)$ is the spectral emittance of the opaque body and $L^{bb}(\lambda, T)$ is the spectral radiance emitted by a blackbody. The latter is represented as

$$L^{bb}(\lambda, T) = \frac{2hc^2}{\lambda^5 \left(e^{hc/\lambda kT} - 1\right)} \tag{2}$$

where

T = the temperature of a blackbody
c = the velocity of light
h = Planck's constant
λ = wavelength
k = Boltzmann's constant

It is clear from these expressions that if the emittance is known, the temperature can be determined by measuring the emitted spectral radiance and inverting Eq. (1). The application of such a measurement procedure to determine the temperature of a water surface exposed to the atmosphere is more complex. The spectral emittance of a sea surface is less than 1 depending upon the emittance angle. Consequently, as one attempts to measure the emitted radiation, some sky radiation will be reflected from the water surface and collected by the infrared sensor. Also, since water does not become opaque to infrared radiation at thermal wavelengths until a depth of approximately 0.10 mm, some of the measured radiation emanates from below the surface, which generally has a slightly different temperature. Therefore, the temperature derived from a measurement of the radiance at the surface will be the temperature of a blackbody which yields an equivalent value of radiance (i. e., the "equivalent radiometric temperature"). It will be different from the actual surface temperature; the degree of difference

1- Temperature accuracies are based upon atmospheric effects only. Other sources of noise and accuracy degradation factors are not included.

will depend upon the magnitude of the reflected radiation and the temperature gradient near the surface.

The present analysis is not concerned with the relationship between the equivalent radiometric temperature and the actual surface temperature, but only with the effect of the atmosphere on the equivalent radiometric temperature derived from a radiometric measurement performed at satellite altitudes. Therefore, all future references to SST will refer to the equivalent radiometric temperature that would be derived from a radiance measurement at the surface.

Before reaching a spaceborne sensor, the spectral radiance emanating from the sea surface will be attenuated by atmospheric constituents, such as clouds, haze, and absorbing gases. These atmospheric constituents also emit and scatter radiant energy, which contributes to the total signal received by the sensor. The central problem in accurately measuring SST from space lies in determining the extent to which such effects can be observed and compensated.

To demonstrate more clearly the nature of the problem of measuring the sea temperature from space, consider the spectral radiance leaving the top of the atmosphere, $L(\lambda)$, which can be represented by:

$$L(\lambda) = L^{bb}[\lambda, T(P_o)]\tau(\lambda, P_o)\epsilon(\lambda) + \int_{\tau(\lambda, P_o)}^{1} L^{bb}[\lambda, T(P)]d\tau(\lambda, P) \qquad (3)$$

where

P_o is surface pressure
τ is atmospheric transmittance
P is atmospheric pressure
T is temperature

According to Eq. (3) estimating $T(P_o)$ from $L(\lambda)$ requires values of temperature, pressure, and the differential absorption properties of the atmosphere. Estimating SST from a single channel radiometric measurement is analogous to inverting Eq. (3) given temperature and pressure values consistent with the prevailing conditions which are obtained from either atmospheric soundings or climatological data.

To eliminate the requirement for ancillary data a scheme was devised which utilizes more than one spectral channel. The scheme was originally discussed and presented by Anding and Kauth [2], and subsequently discussed by McMillin [3] and Prabhakara [4]. The technique, like most remote sounding methods, is based on the use of the differential optical properties of the atmosphere in the infrared window region to infer the atmospheric attenuation. The attenuation values are then used to correct for the effect of the atmosphere on radiometric data.

Theoretical Basis of the Multi-Channel Method

Following the development of Prabhakara [4] the radiative transfer equation may be simplified as:

$$L(\lambda) = L^{bb}[\lambda, T(P_o)]\tau(\lambda, P_o)\epsilon(\lambda) + \overline{L^{bb}}(\lambda)\,[1 - \tau(\lambda, P_o)] \qquad (4)$$

where $\overline{L^{bb}}(\lambda)$ is the weighted mean Planck emission of the atmosphere.

In the infrared window region there are three primary contributors to the absorption. Local water vapor lines, H_2O continuum, and aerosols. The transmission functions for continuum absorption and aerosols are accurately represented by Beers Law. This is also true for selective line absorption when the absorption is either weak or the

individual lines are heavily overlapped. These conditions are approximately satisfied in the window region for one airmass. Hence, window transmission can be expressed as:

$$\tau = e^{-(k_\ell + k_c + k_a)u} = e^{-k_t u} \tag{5}$$

where k_ℓ, k_c, and k_a are the local line, H_2O continuum, and aerosol extinction coefficients, respectively. u is the effective absorber thickness. To a good approximation Eq. (5) can be represented by the first two terms of its series expansion, i.e.,

$$\tau \simeq 1 - k(\lambda)u \tag{6}$$

Substituting (6) into (4), and letting $\epsilon(\lambda) = 1$, we have

$$L(\lambda) \simeq L^{bb}[\lambda, T(P_o)] - \left\{ L^{bb}[\lambda, T(P_o)] - \overline{L^{bb}(\lambda)} \right\} k(\lambda)u \,. \tag{7}$$

Expanding the Planck function about the surface temperature $T(P_o)$ and retaining only the linear term we have

$$L^{bb}[\lambda, T] = L^{bb}[\lambda, T(P_o)] + \frac{\partial L^{bb}[\lambda, T(P_o)]}{\partial T} [T - T(P_o)] \,. \tag{8}$$

This approximation holds for a small wavelength region and a small range of temperatures. This relationship allows Eq. (7) to be expressed as:

$$T(\lambda) = T(P_o) - [T(P_o) - \overline{T}(\lambda)]k(\lambda)u \tag{9}$$

where $T(\lambda)$ is the brightness temperature of the observed radiance, $\overline{T}(\lambda)$ is the equivalent brightness temperature of the atmosphere, and $T(P_o)$ is the surface temperature. Eq. (9) shows a linear relationship between brightness temperature and absorption coefficient, provided $\overline{T}(\lambda)$ is not strongly dependent upon λ over the spectral region. A study by McMillin [3], and results of the present study, show variations of less than 5 per cent. Conceptually, therefore, measurements in only two wavelength intervals for which the respective absorption coefficients are significantly different are required to define the linear relationship.

To demonstrate the concept three wavelength intervals within the infrared window between 10 and 13 μm were chosen. Three intervals were chosen, rather than only two, to observe possible nonlinearities between brightness temperature and absorption coefficient. The intervals chosen were those used by Prabhakara [4], and are respectively, 10.25 - 11.25, 11.25 - 12.0, and 12.0 - 12.9 μm. This result is a consequence of selecting a 1 μm wide interval beginning at the long wavelength side of the 9.6 μm ozone band (the most transparent part of the window region) and then dividing the remaining wavelength interval into two equal wavenumber segments, each 56 cm^{-1} wide.

Absorption coefficient evaluation. - The mean absorption coefficient for each interval was evaluated empirically from transmission spectra computed from an analytical transmission code. For the infrared window region the code utilizes two absorption models; one for H_2O local line absorption and one for H_2O continuum absorption.

Local line absorption is represented by the Goody model [6] which is given by:

$$\tau(\lambda) = \exp\left[\frac{-(S/d)u}{\sqrt{1 + \frac{2}{\overline{P}} \left(\frac{S}{2\pi\alpha}\right) u}} \right] \tag{10}$$

where S/d = intensity to line-spacing parameter (cm^{-1})
u = absorber thickness (pr. cm.)
$\bar{P}$ = Curtis - Godson equivalent pressure (atm)
$\frac{S}{2\pi\alpha}$ = Intensity to half-width parameter (atm . cm^{-1})

The parameters S/d and $S/2\pi\alpha$ were evaluated from a tabulation of spectral line parameters [7] using a procedure discussed by Goody [6], modified to account for an instrument slit function. The parameters were evaluated at a spectral resolution of 10 cm^{-1} defined by the width of the slit function when the transmission is 50%. A comparison between band model and line-by-line derived spectra is shown in Figure 1. Observe that the transmission spectrum is well represented by the Goody model.

Continuum absorption in the window region results from two mechanisms; that caused by the wings of water vapor lines within the 6.3 μm band and the rotational water band which are pressure broadened by foreign gases, and that caused by the same water vapor lines which are self-broadened. The continuum absorption coefficient at total pressure P, and water vapor partial pressure p, is given by:

$$k(P,p) = k_1 P + k_2 p \tag{11}$$

where
k_1 is the absorption coefficient for foreign broadening at unit total pressure;
k_2 is the coefficient for self-broadening at unit water vapor partial pressure.

The values of k_1 and k_2 adapted for the continuum model are based upon a subjective analysis of the data of Bignell [8], Burch [9], and McCoy [10]. The values adopted for k_2 are illustrated in Figure 2. Discussions with Burch and Long indicated that a least-squares fit to the data would yield a self-broadening coefficient that was too high because of systematic errors for the larger data points and because of the consistency of the results of McCoy for the CO_2 lasing line at 10.59 μm. Therefore the selected values coincide with the lowest values shown.

The values adopted for k_1 are based upon the 10.59 CO_2 laser measurements of McCoy [10]. McCoy measured the transmission as a function of total pressure for a fixed water vapor pressure. Using the self-broadening coefficient (k_2) as a basis, the foreign-broadening coefficient (k_1) was determined to be 0.005 k_2.

Both k_1 and k_2 are temperature dependent, the value of k_1 increasing with increasing temperature and the value of k_2 decreasing with increasing temperature. For self-induced absorption the dependence was adopted from the work of Bignell [8] at 2 percent per degree Kelvin. For foreign-induced absorption the temperature dependence was scaled from the temperature dependence of the rotational water lines at 2 percent per degree Kelvin.

The empirical evaluation of the absorption coefficients was accomplished as follows. Ten atmospheric representations of temperature and humidity were selected from the NASA Four-Dimensional Model Atmosphere compilation [11], representing moist and dry conditions ($\pm$ one standard deviation from mean moisture conditions) for five oceanic global regions extending from the North Sea to the equator. These atmospheric data were input to the transmission code and spectral transmission from 10 to 13 μm was computed. These values were integrated over the respective wavelength intervals and transmission versus effective absorber thickness was plotted. The result is presented in Figure 3. Assuming transmission is accurately represented by Beers Law, i. e., $\tau = \exp(-ku)$, linear least squares fits to $\ln\tau$ versus u yielded three respective values for the absorption coefficient, which are also given in Figure 3.

To demonstrate the relationship between brightness temperature and absorption coefficient, the ten model atmospheres were input to atmospheric radiance codes and the vertical upwelling radiance at space altitudes, emanating from a sea surface whose temperature equaled $T(P_o)$ was calculated. To establish realism to the computations, and to add an additive source of noise, aerosol effects were included in the calculations. Specifically, two aerosol representations were selected, taken from the work of Fenn [12]. One whose optical properties and size distribution were consistent with a 100 percent maritime haze and the other with a 60 percent maritime haze and a 40 percent continental haze. The altitude distribution of aerosol density was assumed variable and controlled by the sea-level visibility. A 23 km visibility was used for the maritime haze, a 10 km visibility for the maritime-continental haze. The calculations of radiance were made by numerically evaluating Eq. (3), using the infrared window transmission described above to evaluate $d\tau(\tau, P)$. For each of the twenty spectra, in-band brightness temperatures were evaluated and plotted versus absorption coefficient. The results are shown in Figure 4a - 4e. The straight lines are least squares fits to the data.

Discussion of results. - Observe that a nonlinearity exists between brightness temperature and absorption coefficient, which diminishes at higher brightness temperatures. This occurs because the atmospheric brightness temperature increases approximately 5 percent at the longer wavelength regions, and the increase is observable at the lower brightness temperatures, but becomes nearly insignificant for brightness temperatures above 290° K. Also note that the atmosphere causes a decrease in the observed brightness temperature of the sea surface ranging from 2° K for the cool northern region to greater than 5° K for the warm equatorial region. The application of the technique does, however, estimate the input SST values to within $\pm$ 0.5° K. Furthermore, the 3-band estimate is insignificantly better than the 2-band estimate ($\pm$ 0.5° K compared to $\pm$ 0.3° K).

The application of the technique to actual space-acquired data is shown in Figures 5 and 6. For each of the six cases the brightness temperatures were taken from Prabhakara [4], which were measured by the IRIS instrument on Nimbus 4. Observe nearly perfect linearity is demonstrated and that excellent agreement is obtained between predictions and ship measurements for three of the cases (Figure 5). The reason for the discrepancy for the other three cases (Figure 6) is unknown, although it could be attributable to a decrease in surface emissivity resulting from a high sea state.

The utilization of Skylab EREP S191 data as a verification experiment fell far short of expectations because of instrument problems. Although the problems have been identified, their effects remain uncorrected. Of the eight test areas planned for usage only one gave results which were considered satisfactory. This was for the Monroe Reservoir on 10 June 1973. A circumstance of the spectrometer was that whenever the brightness temperature of the spectral radiance was significantly different than either the ambient calibration source temperature, or the temperature of the internal mirrors or dichroic, inaccurate data resulted. For the Monroe Reservoir the aperture brightness temperature was approximately equal to the internal instrument temperatures and accurate data were obtained.

During the overpass of EREP the surface temperature was measured with a Barnes PRT5 radiometer yielding an average value of 25° C. Also, temperature and humidity data were obtained by a local radiosonde. Both the surface temperature and radiosonde data were input to the radiative transfer model and the radiance at the S191 aperture was calculated. Also included in the calculation was a 23 km visibility continental haze. A comparison of measured and calculated radiance is presented in Figure 7. Generally, the agreement is very good. Minor differences are noted between 8 and 9 μm, probably caused by the reduced values of aperture brightness temperature. Of major concern for

the present study is the region between approximately 10.5 and 13.0 μm, where the agreement is within a few percent. It would appear from this comparison that the radiative transfer model is a reasonable representation of reality.

To examine the application of the SST estimation technique to this data, for both the EREP spectra and the model calculations, the inband brightness temperatures were computed and plotted versus absorption coefficient. Least-squares lines were fitted to the data and the results are shown in Figure 8. Observe that both the model calculations and the EREP data estimate a surface temperature within $\pm$ 1.0^{o} K of the recorded ground truth temperature.

CONCLUSIONS AND RECOMMENDATIONS

The results presented herein indicate that a significant benefit will be derived by the addition of a second channel in the infrared window region. Specifically, atmospheric-effect uncertainties can probably be reduced to less than 1.0^{o} K without recourse to climatological data. The technique is likely to produce a significant benefit for unusual conditions, such as warm moist atmospheres over cool waters or vice versa, when climatological data would yield a particularly poor result.

The results presented herein are based upon a study of limited scope, with recourse to a limited amount of data. Although the study results are indicative, it would be desirable to apply the technique to a broader data base before a final choice is made for the spectral bands to be used in the latter satellites of the TIROS-N series.

REFERENCES

1. W. L. Smith, P. K. Rao, R. Koffer and W. R. Curtis, "The Determination of Sea-Surface Temperature from Satellite High Resolution Infrared Window Radiation Measurements," Monthly Weather Review, Vol. 98, No. 8, Aug. 1970, pp. 604-611.
2. D. Anding and R. Kauth, "Estimation of Sea-Surface Temperature from Space," Remote Sensing of Environment, Vol. 1, 1970, pp. 217-220.
3. L. McMillin, A Method of Determining Surface Temperature from Measurements of Spectral Radiance at Two Wavelengths, Ph. D. dissertation, Iowa State University, 1971.
4. C. Prabhakara, B. Conrath, and V. Kunde, Estimation of Sea-Surface Temperature from Remote Measurements in the 11 - 13 μm Window Region, Goddard Space Flight Center, Greenbelt, MD, 1972.
5. J. Price, Analysis of Some Methods for Obtaining Sea-Surface Temperatures from Satellite Observations, Goddard Space Flight Center, Greenbelt, MD, 1973.
6. R. M. Goody, Atmospheric Radiation, I Theoretical Basis, Oxford at the Clarendon Press, 1964.
7. R. McClatchey, AFCRL Atmospheric Absorption Line Parameters Compilation, AFCRL, L. G. Hanscom Field, Bedford, Mass., AFCRL-TR-73-0096, Jan. 1973.
8. K. Bignell, Quar. Jour. Roy. Met. Soc., Vol. 96, 1970, p. 390.
9. D. Burch, Investigation of the Absorption of Infrared Radiation by Atmospheric Gases, Philco-Ford Corporation, Aeronutronic Division, Rept. No. U-4784, January 1970.
10. J. McCoy, D. Rensch and R. Long, Applied Optics, Vol. 8, No. 7, 1969.

11. D. Spiegler and J. Greaves, Development of Four-Dimensional Atmospheric Models (Worldwide), Allied Research Associates, Inc., Concord, Mass., NASA CR-61368, August 1971.

12. R. Fenn, Private Communications, AFCRL, Bedford, Mass., 1975.

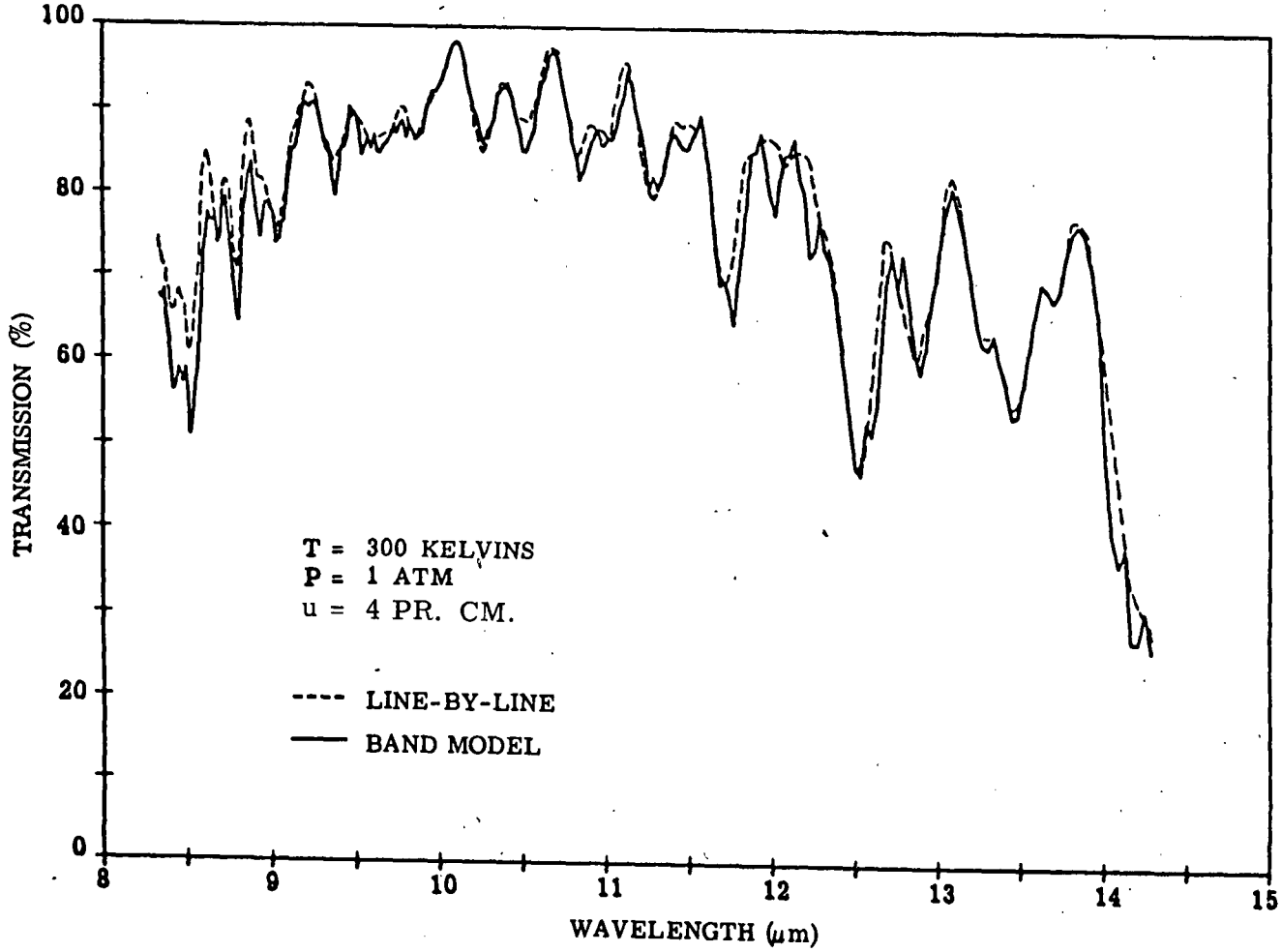

Figure 1. A Comparison of Band Model and Line-by-Line Derived Spectra for H_2O Local Line Absorption in the Infrared Window Region.

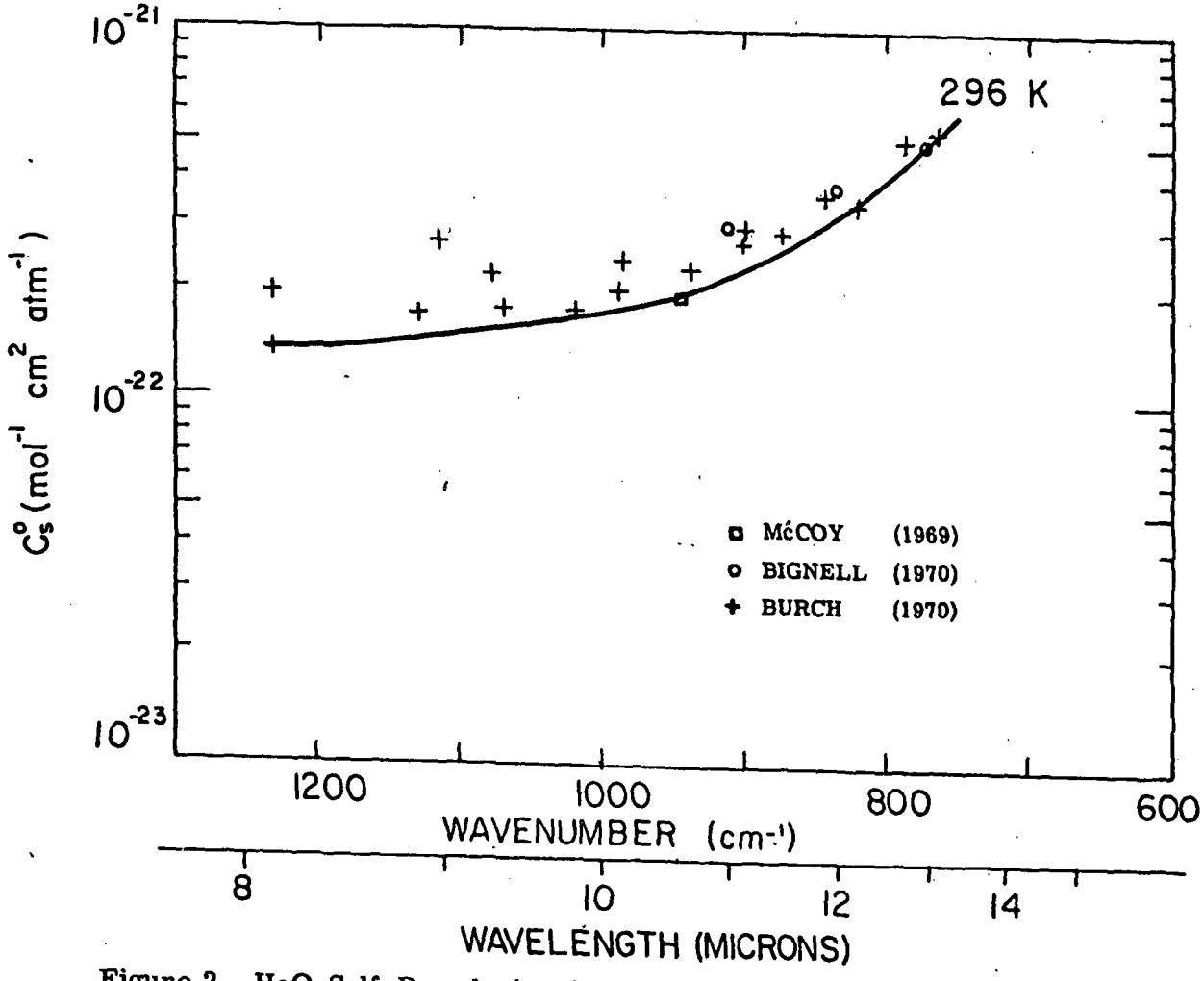

Figure 2. H_2O Self-Broadening Continuum Absorption Coefficient for Infrared Window Region.

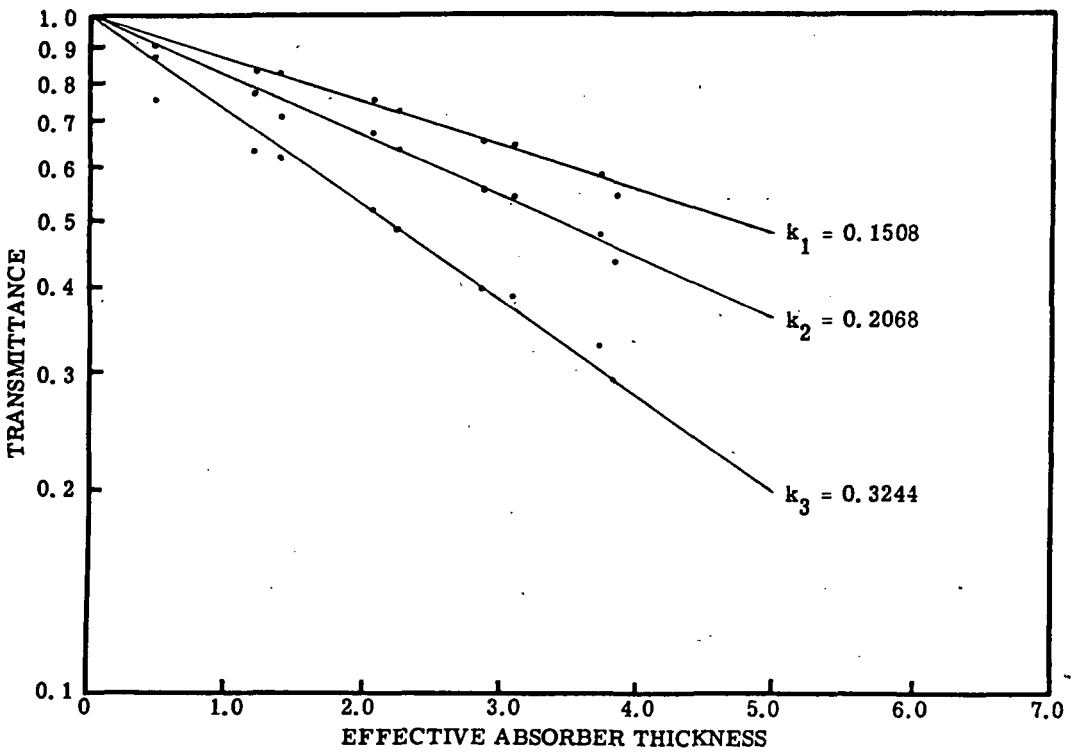

Figure 3. Average Transmission Versus Effective Absorber Thickness for Three Wavelength Regions (10.25 - 11.25, 11.25 - 12.0, 12.0 - 12.9 μm). k_1, k_2, k_3 are the respective Beers Law Absorption Coefficients.

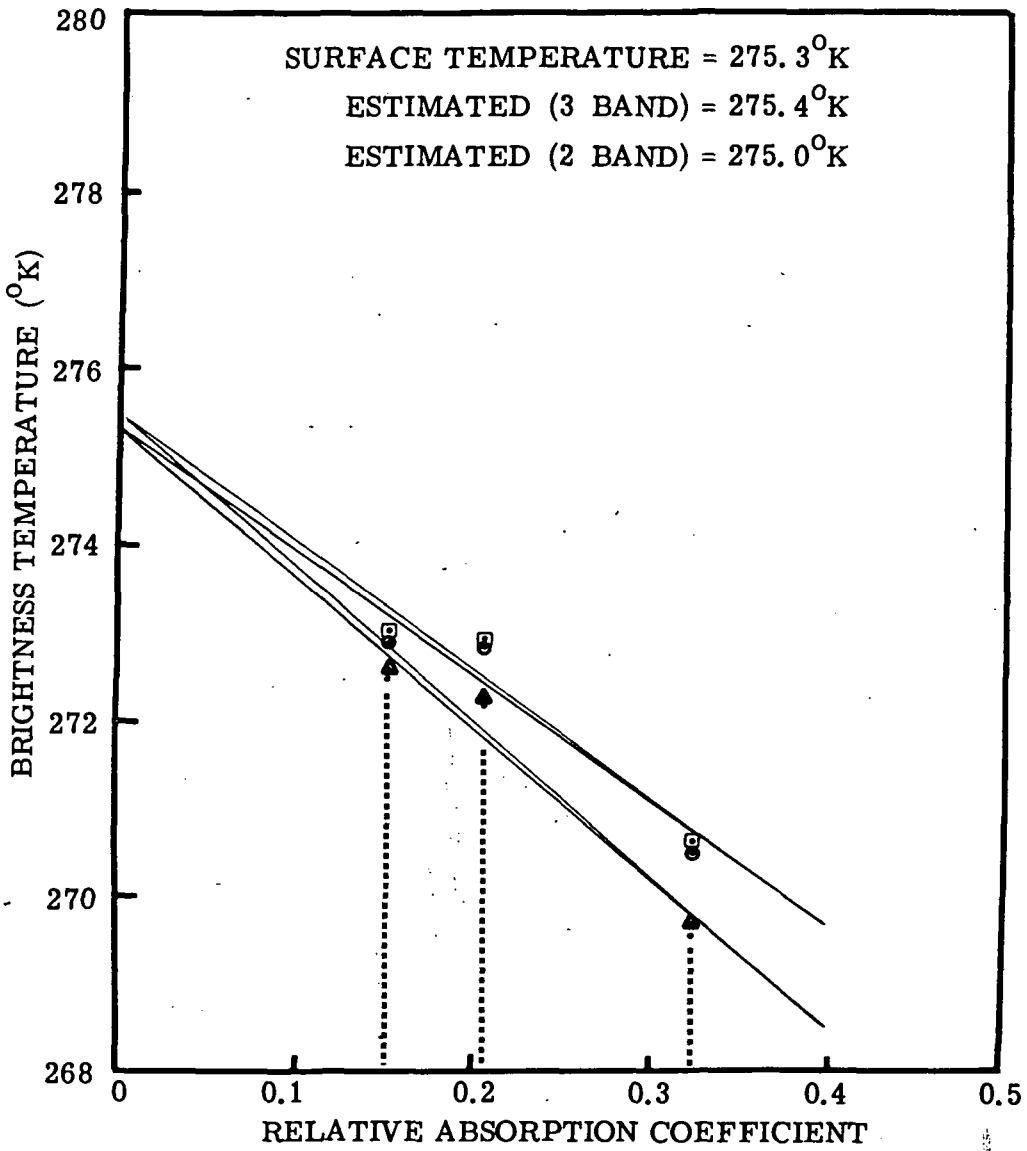

Figure 4a. Brightness Temperature Versus Absorption Coefficient.
Key: ⊡ Low Humidity, Continental-Maritime Haze;
● Low Humidity, Maritime Haze;
▲ High Humidity, Continental-Maritime Haze;
· High Humidity, Maritime Haze.

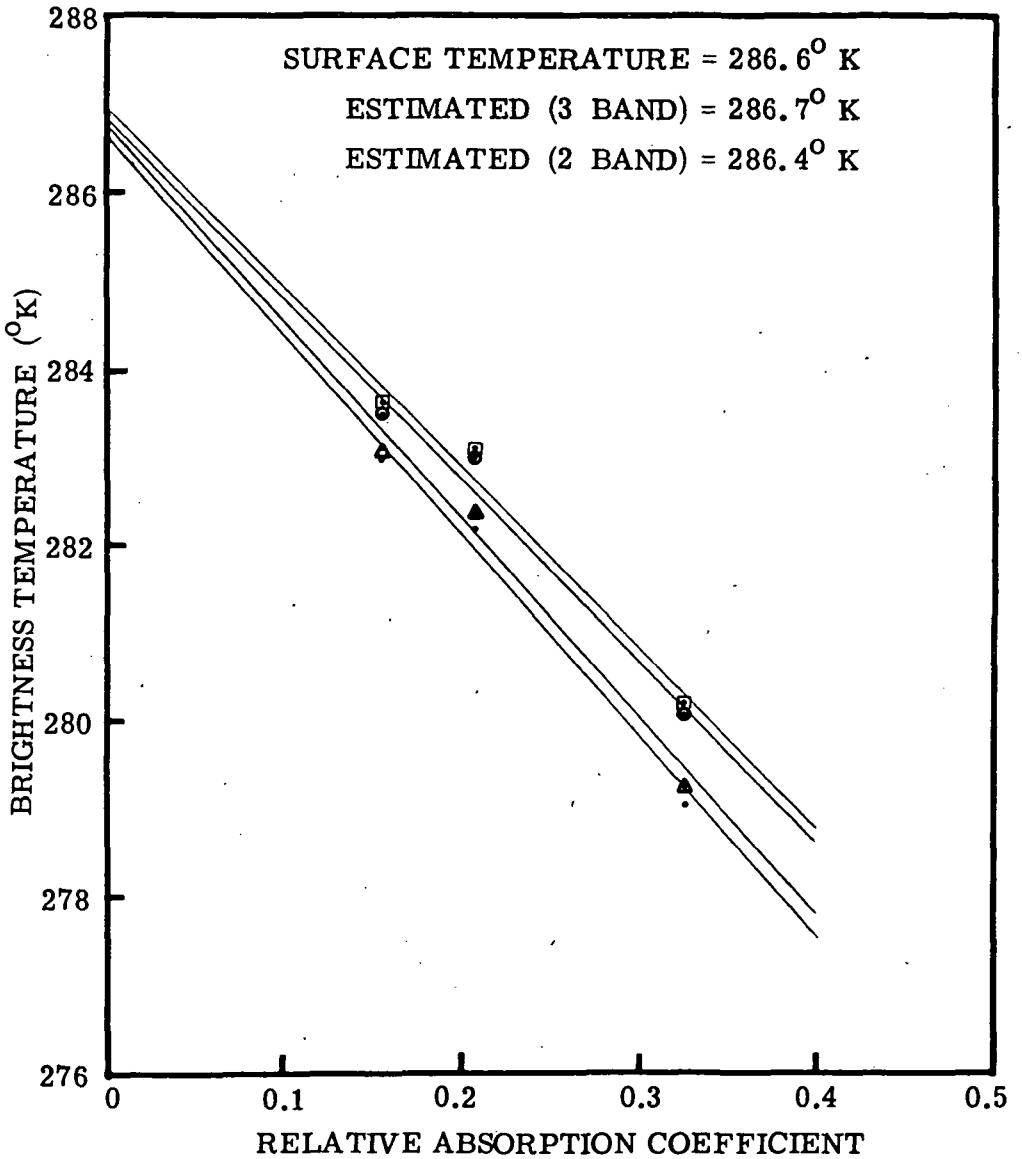

Figure 4b. Brightness Temperature Versus Absorption Coefficient.
Key: ▫ Low Humidity, Continental-Maritime Haze;
● Low Humidity, Maritime Haze;
▲ High Humidity, Continental-Maritime Haze;
· High Humidity, Maritime Haze.

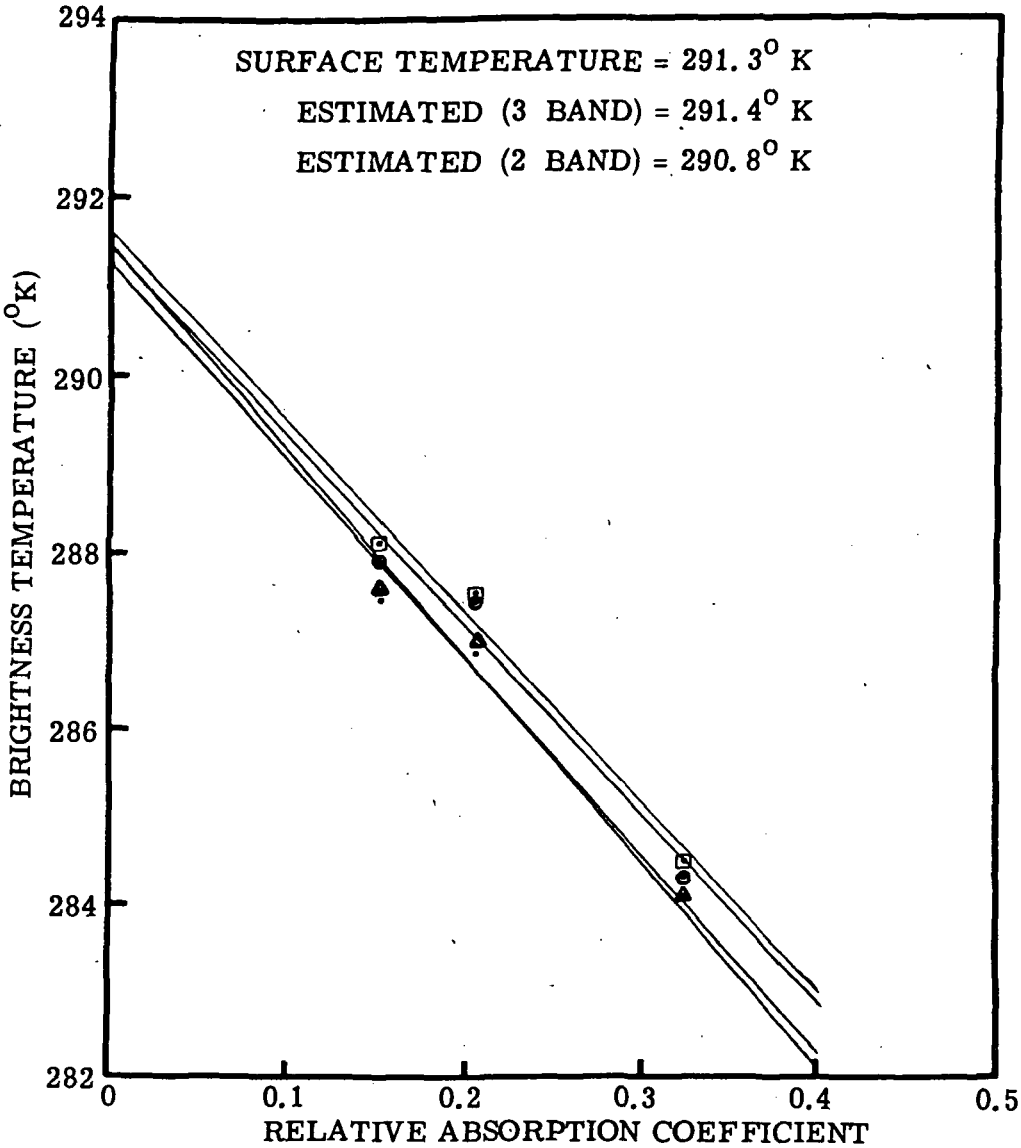

Figure 4c. Brightness Temperature Versus Absorption Coefficient.
Key: ⊡ Low Humidity, Continental-Maritime Haze;
● Low Humidity, Maritime Haze;
▲ High Humidity, Continental-Maritime Haze;
· High Humidity, Maritime Haze.

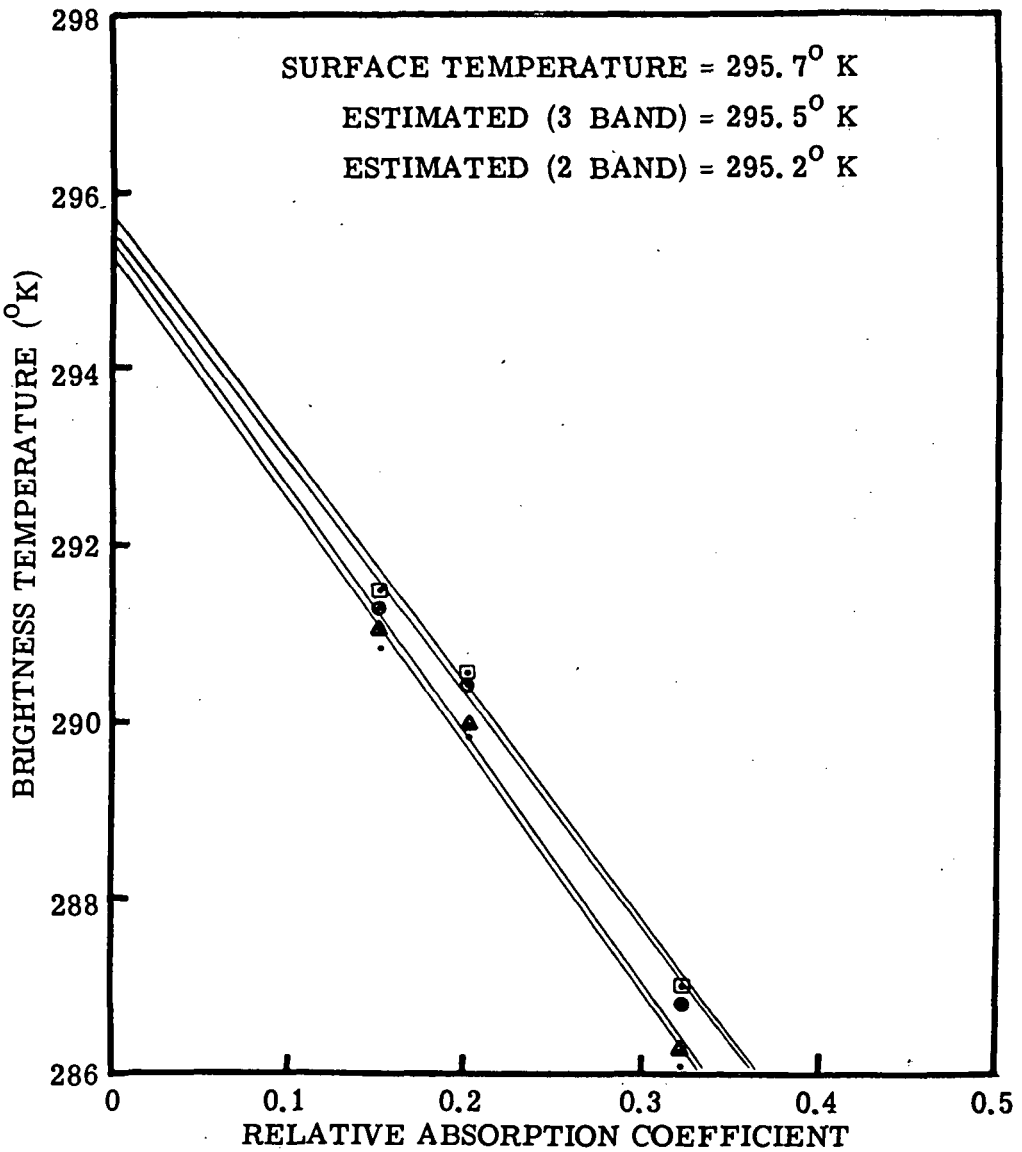

Figure 4d. Brightness Temperature Versus Absorption Coefficient.
Key: ⊡ Low Humidity, Continental-Maritime Haze;
⊙ Low Humidity, Maritime Haze;
△ High Humidity, Continental-Maritime Haze;
. High Humidity, Maritime Haze.

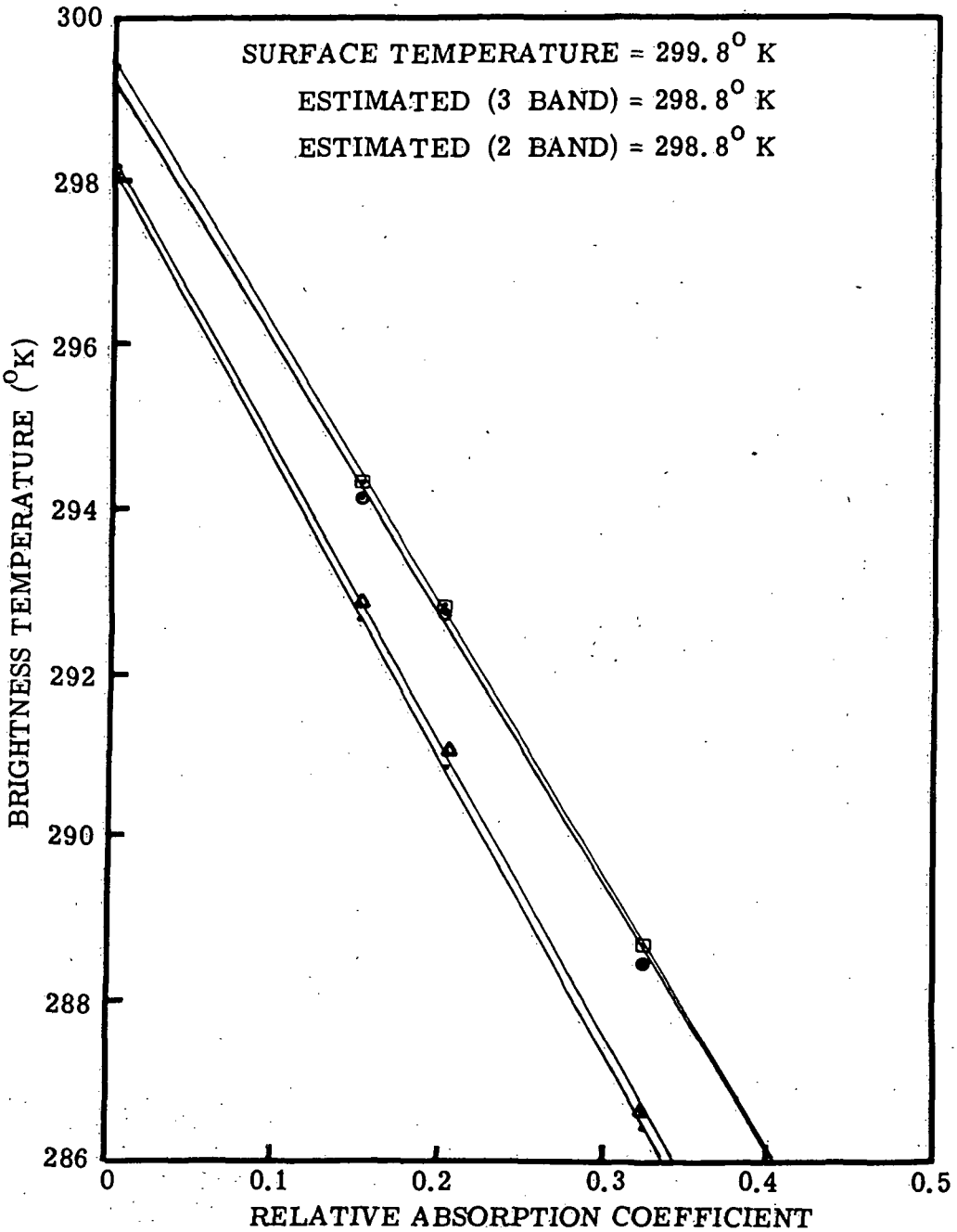

Figure 4e. Brightness Temperature Versus Absorption Coefficient.
Key: ⊡ Low Humidity, Continental-Maritime Haze;
⊙ Low Humidity, Maritime Haze;
▲ High Humidity, Continental-Maritime Haze;
△ High Humidity, Maritime Haze.

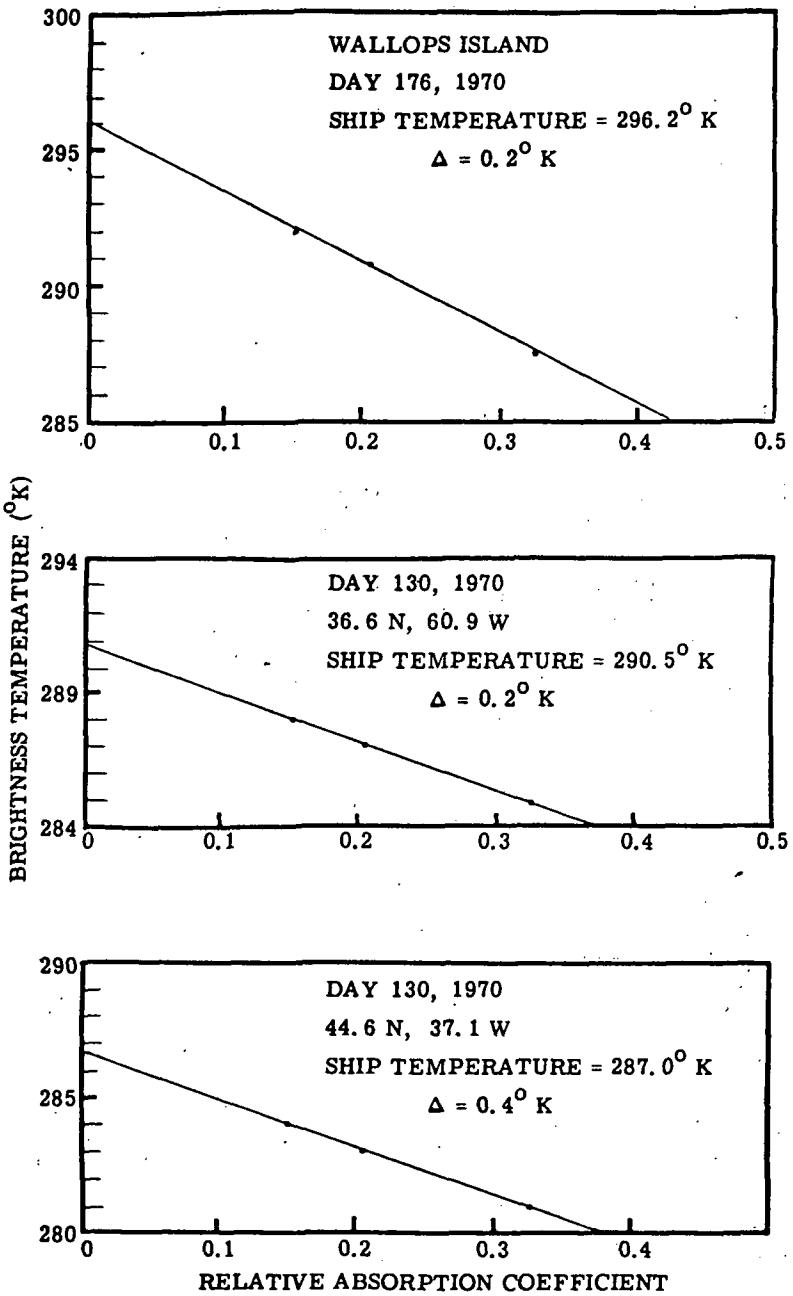

Figure 5. IRIS Measured Brightness Temperature Versus Relative Absorption Coefficient.

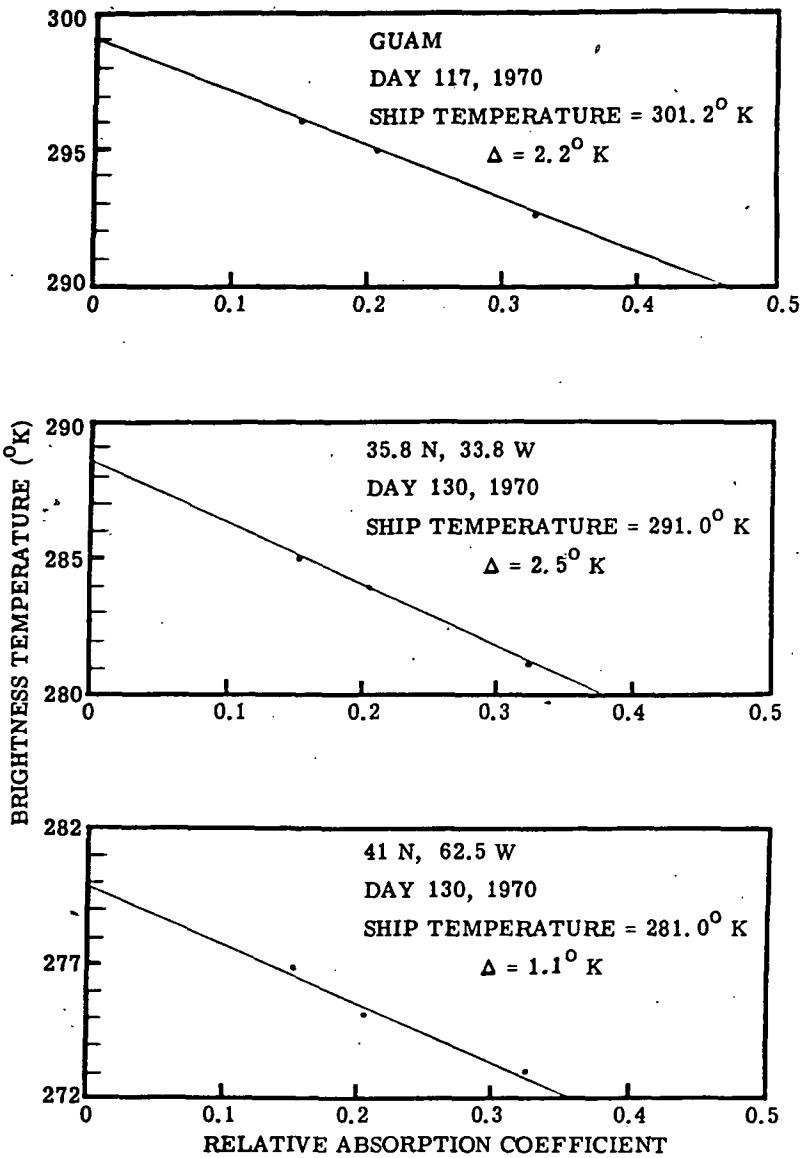

Figure 6. IRIS Measured Brightness Temperature Versus Absorption Coefficient.

1971

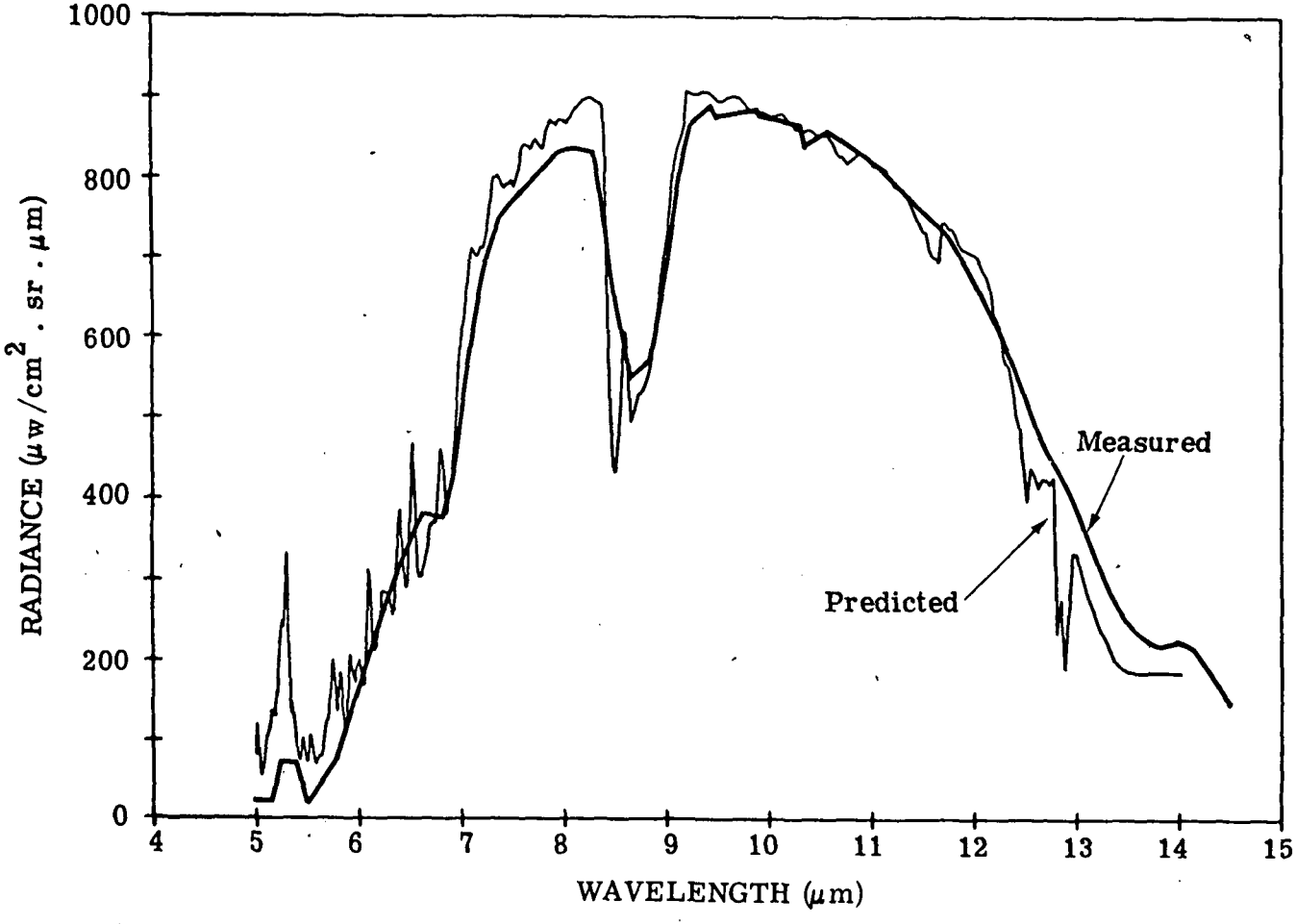

Figure 7. Comparison of Measured and Predicted Spectral Radiance for Monroe Reservoir, Salem, Illinois, on 10 June 1973. Water Surface Temperature = 298° K.

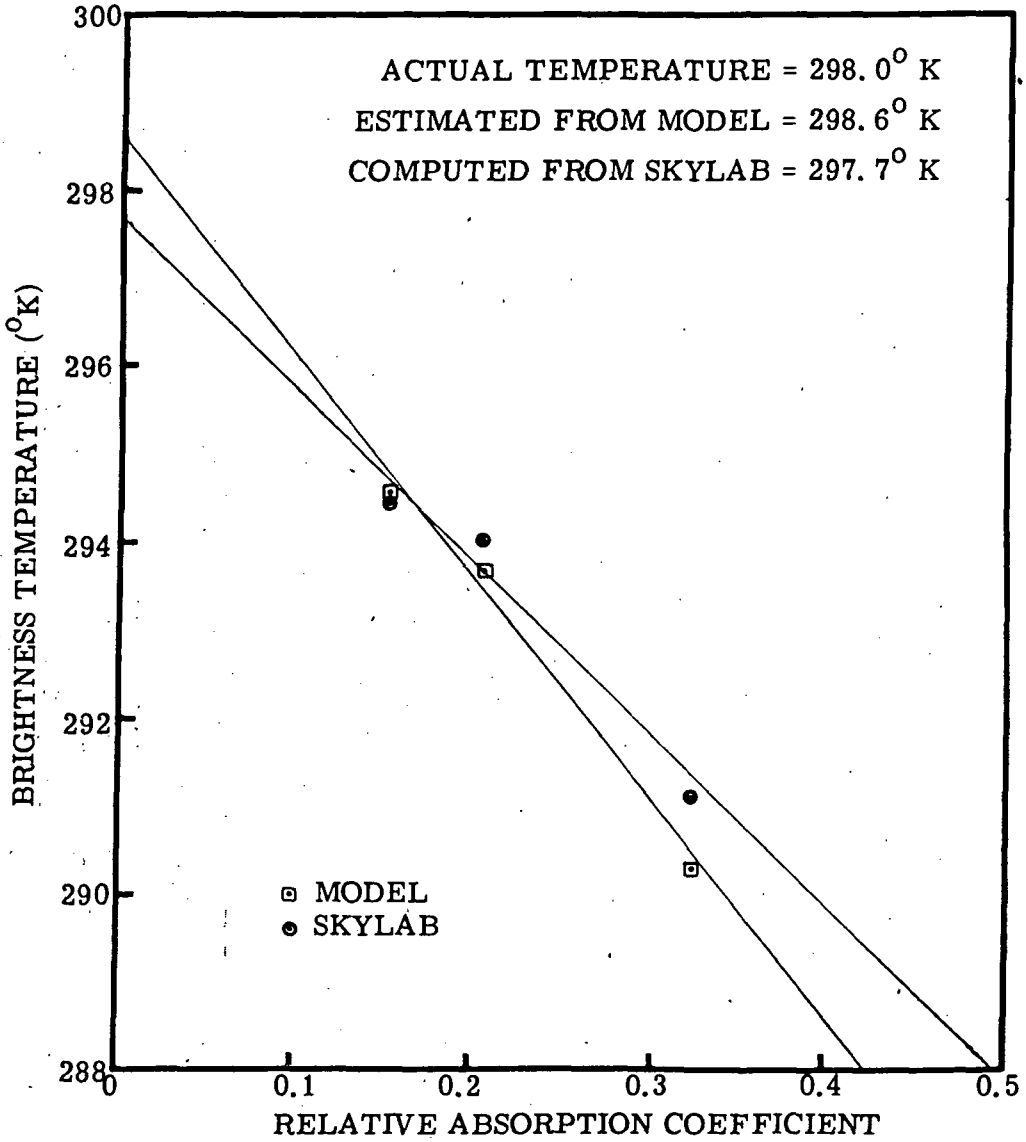

Figure 8. Brightness Temperature Versus Absorption Coefficient for Monroe Reservoir on 10 June 1973. Model Predictions Compared to S191 Measurement Predictions.